Progress In Electromagnetics Research M, Vol. 82, 195–203, 2019

Design of a Broadband Circularly Polarized Antenna Array

Zhengyan Lu, Le Yang, and Lingsheng Yang*

Abstract—A broadband circularly polarized antenna array is proposed in this paper. The array consists of four sequentially rotated feed groove-backed strip antennas. Compact size (46 mm × 46 mm × 1.6 mm), wide impedance bandwidth (4.62–9.92 GHz), and wide 3 dB axial ratio bandwidth (4.48–8.52 GHz) can be observed. The measured peak gain is 7.5 dBi at 8.2 GHz, and good agreement between the simulated and measured results can be achieved.

1. INTRODUCTION

Due to the advantages of being robust to multipath fading [1], higher gain [2], and improvement in radiation performances [3], circularly polarized array antennas are widely used in modern wireless communication systems such as satellite, radar, and mobile communication. However, it is always a challenging task for circularly polarized antenna arrays to achieve broad bandwidth with compact size, simple structure, and light weight.

Among all the circularly polarized antenna array designs, sequentially feed array is very attractive, because it can obtain a wide axial ratio with a simple structure [4]. In [5], the circularly polarized square-slot antenna array designed by using sequential rotation feed structure can achieve an impedance bandwidth of 51.9% and an axial ratio bandwidth of 31.4%. In [6], a non-resistive series (sequential rotation) feed network is used to form a compact circularly polarized microstrip antenna array for airborne communication. The final impedance bandwidth is 22.4%, and the 3 dB axial ratio bandwidth is only 6.8%. Sequentially rotated feed technology is also used in [7] to form a broadband circularly polarized slot antenna array with an impedance bandwidth of 52% and an axial ratio bandwidth of 52%. A sequentially phased network is applied in [8], and a broadband directional circularly polarized antenna array with an impedance bandwidth of 40% and an axial ratio bandwidth of 36.6% can be achieved. In [9], a similar feed network is used to design a circularly polarized corner-truncated patch array antenna, and the array can obtain a 39% impedance bandwidth and a 27.6% axial ratio bandwidth. In [10], sequentially rotated series-parallel feed is used to realize a 31.1% axial ratio bandwidth based on a circularly polarized array of super-surfaces.

In this paper, a sequentially rotated feed circular polarized antenna array with broadband performances is proposed. According to the experimental results, the −10 dB impedance bandwidth is 72.9% (4.62–9.92 GHz), and a 3 dB axial ratio bandwidth is 62.2% (4.48–8.52 GHz). The paper is arranged as follows. In Section 2, a broadband circularly polarized antenna element is designed in detail. In Section 3, the element is used to form a four-element antenna array. The array is fabricated and measured in Section 4. Finally, conclusion is made in Section 5.

Received 14 April 2019, Accepted 22 May 2019, Scheduled 8 July 2019

* Corresponding author: Lingsheng Yang (ylsinchina@163.com).

The authors are with the Department of Electronics & Information Engineering, Nanjing University of Information Science & Technology, No. 219, Ningliu Road, Nanjing, China.

2. ANTENNA ELEMENT DESIGN

The proposed antenna element is shown in Fig. 1. The antenna is mounted on a 1.6 mm thick FR4 substrate ($\varepsilon_r = 4.4$, loss tangent of 0.02). The ground plane with a circular groove is set at the back of the substrate. The feed structure is based on a rectangular strip. In order to miniaturize the antenna and realize circular polarization performances, two trapezoidal strips are attached to the rectangular strip. Two symmetrical rectangular slots are extended from the circular groove, and the axial ratio of the element can be further increased. The total size of the antenna is $18 \times 18 \times 1.6\,\text{mm}^3$, and the detailed parameters of the antenna are listed in Table 1.

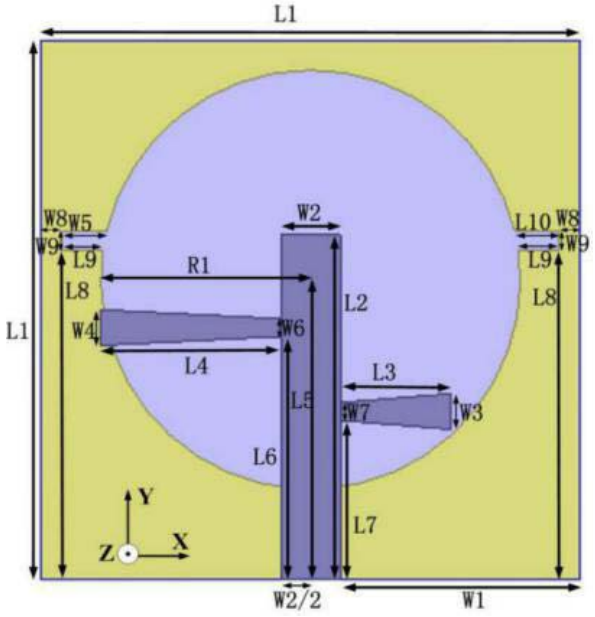

Figure 1. Configuration of the proposed antenna.

Table 1. Detailed values of the antenna parameters (mm).

$L1$	18	$L8$	11	$W6$	0.6
$L2$	11.5	$L9$	1.4	$W7$	0.6
$L3$	3.7	$W1$	8	$W8$	0.7
$L4$	6	$W2$	2	$W9$	0.6
$L5$	10	$W3$	1.2	h	1.6
$L6$	8.1	$W4$	1.2	$R1$	7
$L7$	5.3	$W5$	1.5	$L10$	1.5

The design process of the antenna element is divided into three steps (Fig. 2): In step 1, the antenna consists of a ground plane with a circular groove, and a simple feeding structure contains a rectangular strip with two subsidiary rectangular branches. In step 2, the two subsidiary rectangular branches are replaced by two trapezoidal branches. In step 3, two symmetrical rectangular slots are extended from the circular groove. The structures from steps 1–3 are simulated by using the High Frequency Structure Simulation (*HFSS*) software version 15.0 (*Ansys Corp.*). The simulated impedance bandwidth and axial ratio bandwidth curves are shown in Fig. 3. For Antenna_1, the impedance bandwidth is 5.81–8.76 GHz, and the axial ratio bandwidth is 5.83–7.83 GHz. The two rectangular branches are used to obtain circularly polarized performances. For Antenna_2, the impedance bandwidth is 5.24–8.1 GHz,

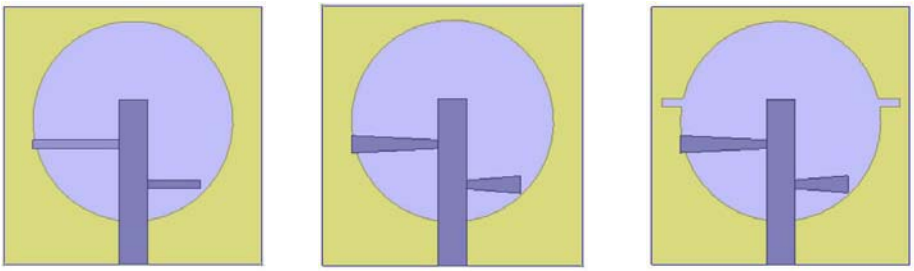

(a) Antenna_1 (b) Antenna_2 (c) Antenna_3

Figure 2. Antenna evolution process. (a) Step 1, (b) step 2, (c) step 3.

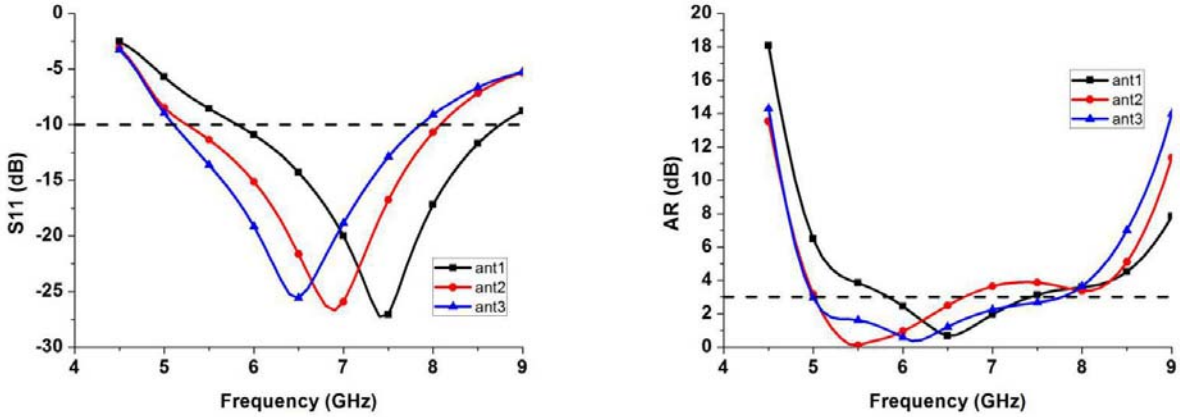

(a) (b)

Figure 3. Simulated results of steps 1–3. (a) Impedance bandwidth, (b) axial ratio bandwidth.

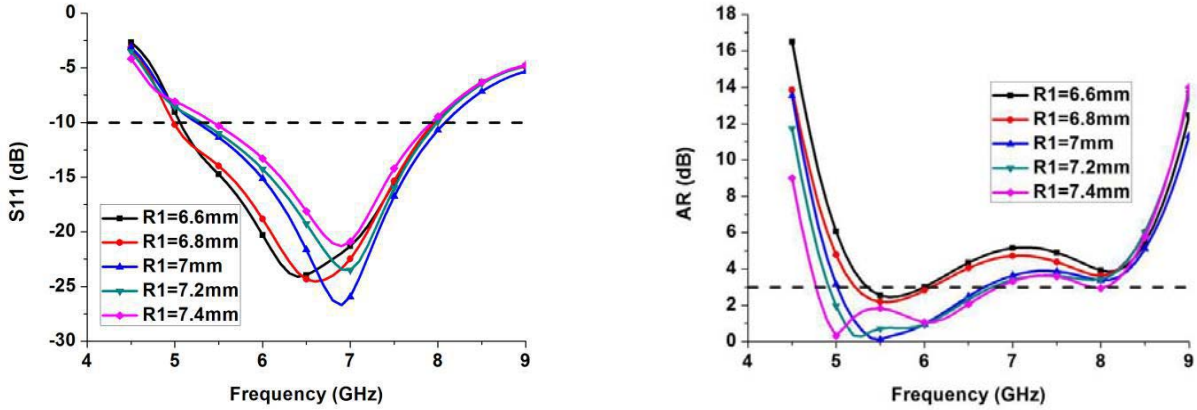

(a) (b)

Figure 4. Affect of circular groove on impedance bandwidth and axial ratio bandwidth.

and the axial ratio bandwidth is 5.02–6.74 GHz. By changing the shape of the two branches, the band shift to lower frequency and the size of the antenna can be miniaturized accordingly. For Antenna_3, the impedance bandwidth is 5.1–7.88 GHz, and the axial ratio bandwidth is 5–7.78 GHz. When Antenna_1 is transformed to Antenna_2, the impedance bandwidth and axial ratio bandwidth shift to the lower frequency. When Antenna_2 is changed to Antenna_3, the impedance bandwidth shifts slightly, while the impedance bandwidth is almost unchanged, but the axial ratio bandwidth becomes much wider. So

the two extended slots can be used to enhance the circular polarization performances.

Figure 4 shows how the radius of the circular groove ($R1$) affects the impedance bandwidth and axial ratio bandwidth. It can be found that as $R1$ increases, the lower frequency of impedance bandwidth gradually shifts to the higher frequency; meanwhile, the lower frequency of the axial ratio bandwidth also gradually shifts to the lower frequency; however, the upper frequencies of the impedance bandwidth and axial ratio bandwidth are nearly unchanged. Considering the impedance bandwidth and axial ratio bandwidth, the final $R1$ is chosen as 7 mm.

By setting the observation plane about 12.5 mm above the top surface of the antenna, the electric field vector at 6 GHz can be observed. As can be seen in Fig. 5, the electric field vector rotates counterclockwise, which indicates that the antenna performs right-handed circularly polarized (RHCP) radiation.

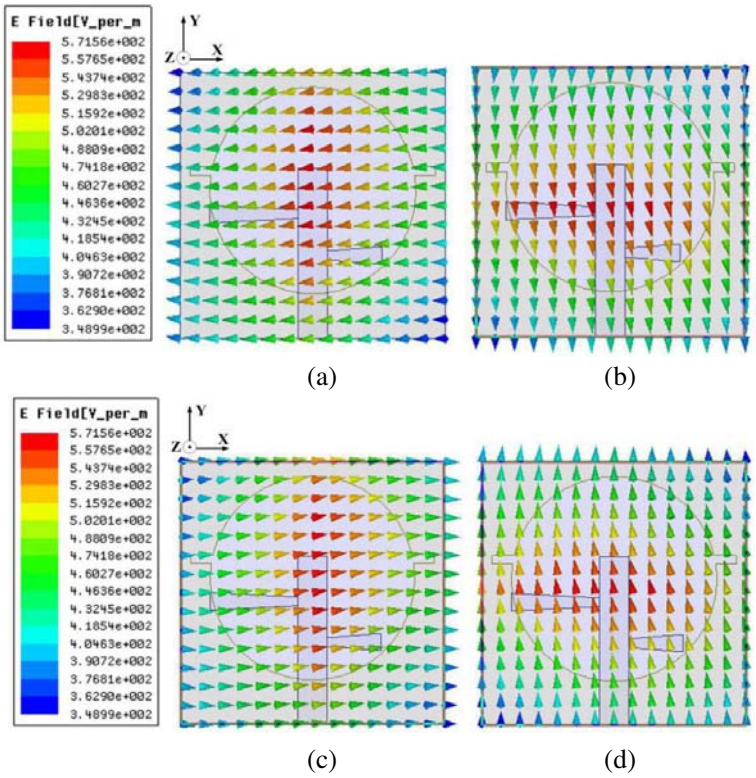

Figure 5. Electric field vector at different phases at 5.8 GHz. (a) 0°, (b) 90°, (c) 180°, (d) 270°.

3. ARRAY DESIGN

Figure 6 shows the geometry of the proposed 2 × 2 array. The feed network is an open square ring. The four elements are arranged in a sequentially rotating configuration and connected to the feed network by four rectangular strips located at the four corners. The proposed array has an overall size of $46 \times 46 \times 1.6\,\text{mm}^3$. The detailed configurations of the array are listed in Table 2.

Figure 7 is a schematic diagram of the feed network. Port 1 is the input terminal, and Port 2, Port 3, Port 4, and Port 5 are the four output terminals connected with the four elements. $Z0$ represents the characteristic impedance (50 ohm), and $Z1$, $Z2$, and $Z3$ represent the impedances of the quarter-wavelength strips (Line 1, Line 2, Line 3, Fig. 6), respectively. $Z4$ is the impedance of the output terminal. Ports 2 to 5 are located as shown in Fig. 6. When the phase at Port 2 is set as deg (phase reference), the phase differences of deg-90°, deg-180°, and deg-270° will appear at the output Ports 3 to 5, accordingly.

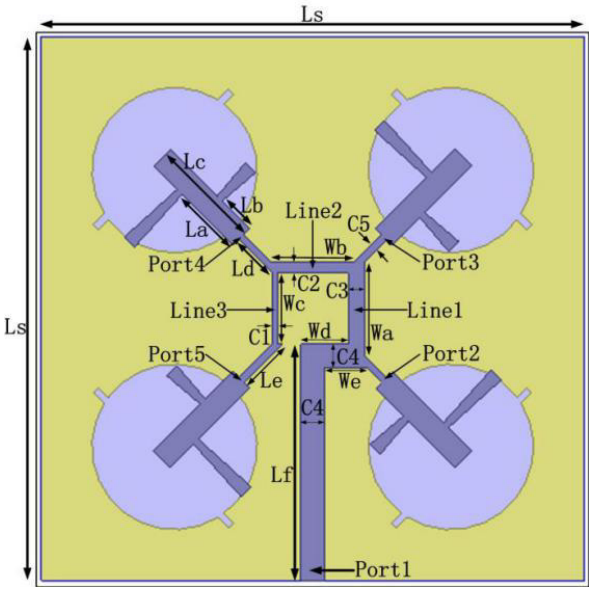

Figure 6. 2×2 antenna array structure.

Table 2. Detailed values of array antenna parameters (mm).

La	6.1	Wb	7	$C4$	2
Lb	3.3	Wc	6	$C5$	0.6
Lc	9.5	Wd	4	Ls	46
Ld	4	We	3.6	h	1.6
Le	4.6	$C1$	0.4		
Lf	20	$C2$	0.9		
Wa	8	$C3$	1.4		

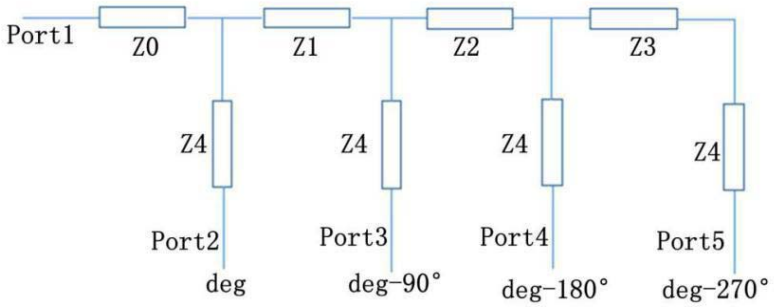

Figure 7. Schematic diagram of the feed network.

4. MEASUREMENT AND RESULTS

In order to study the performance of the array in practical applications, the antenna array is fabricated (Fig. 8) and measured by using Agilent N9918A in an anechoic chamber. As shown in Fig. 9, the measured impedance bandwidth agrees well with the simulated results. The simulated -10 dB impedance bandwidth is from 4.61 GHz to 10.15 GHz, while the measured -10 dB impedance bandwidth is from 4.62 GHz to 9.92 GHz. The differences are mainly due to dielectric loss and manufacturing error.

(a) (b)

Figure 8. Fabricated antenna array. (a) Top view. (b) Bottom view.

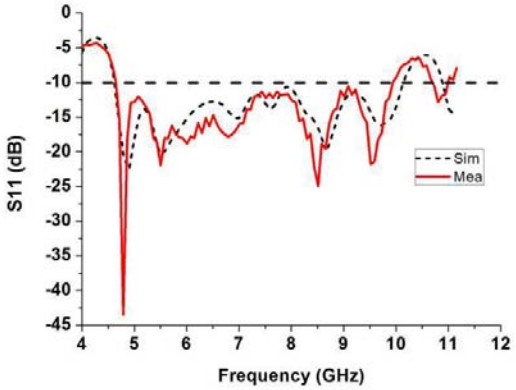

Figure 9. Simulated and measured impedance bandwidth of the proposed array.

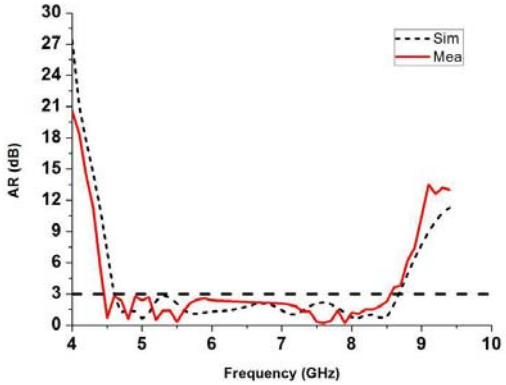

Figure 10. Simulated and measured 3 dB axial ratio bandwidth.

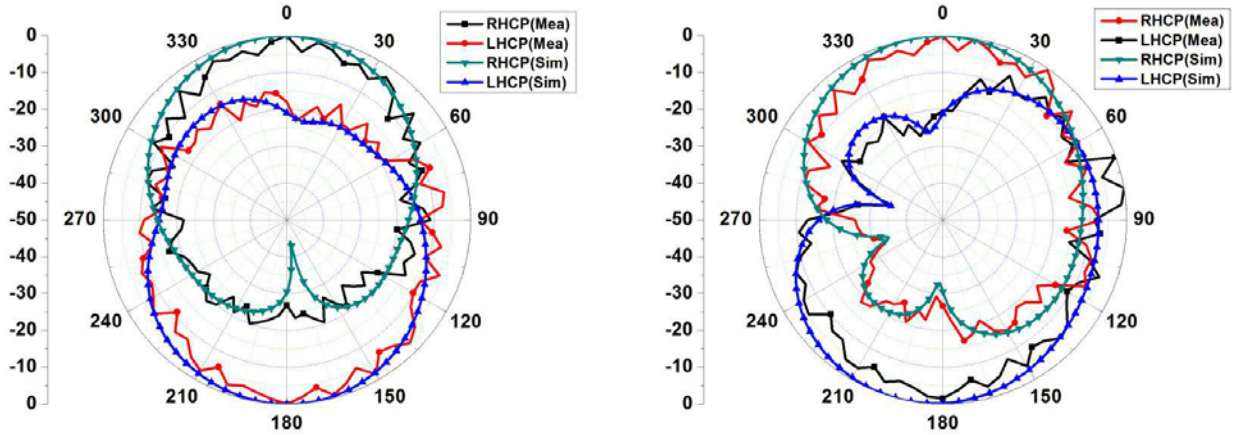

(a) (b)

Figure 11. Simulated and measured radiation patterns at 5.8 GHz, (a) xz-plane, (b) yz-plane.

Fig. 10 shows the measured and simulated 3 dB axial ratio bandwidths. The measured 3 dB axial ratio bandwidth varies from 4.48 GHz to 8.52 GHz. It can also be observed from Fig. 10 that compared with simulated results, the measured results slightly shift to the lower frequency.

The simulated and measured radiation patterns at 5.8 GHz in xz-plane and yz-plane are plotted in Fig. 11. As can be seen from this figure, RHCP radiation is in the $+Z$ direction, and LHCP radiation can be observed in the $-Z$ direction.

Figure 12 shows the simulated and measured maximum gains of the array antenna. It can be seen from this figure that the measured maximum gain is 7.5 dBi at 8.2 GHz.

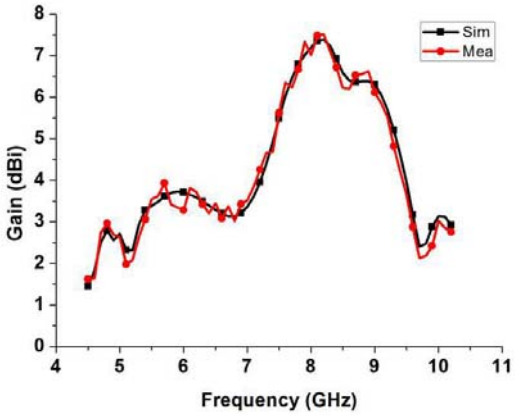

Figure 12. Simulated and measured gains of the array.

Figure 13 shows the surface current distribution of the array at 5.8 GHz. It can be observed that the direction of the vector sum of surface distributed currents on the radiating element is rotated counterclockwise. The results show that the proposed array exhibits right-handed circular polarization (RHCP) in the $+z$ direction. Also coupling between antenna elements can be found (the distortion of current distribution between antenna elements). This explains why the array has a wider bandwidth than the single element.

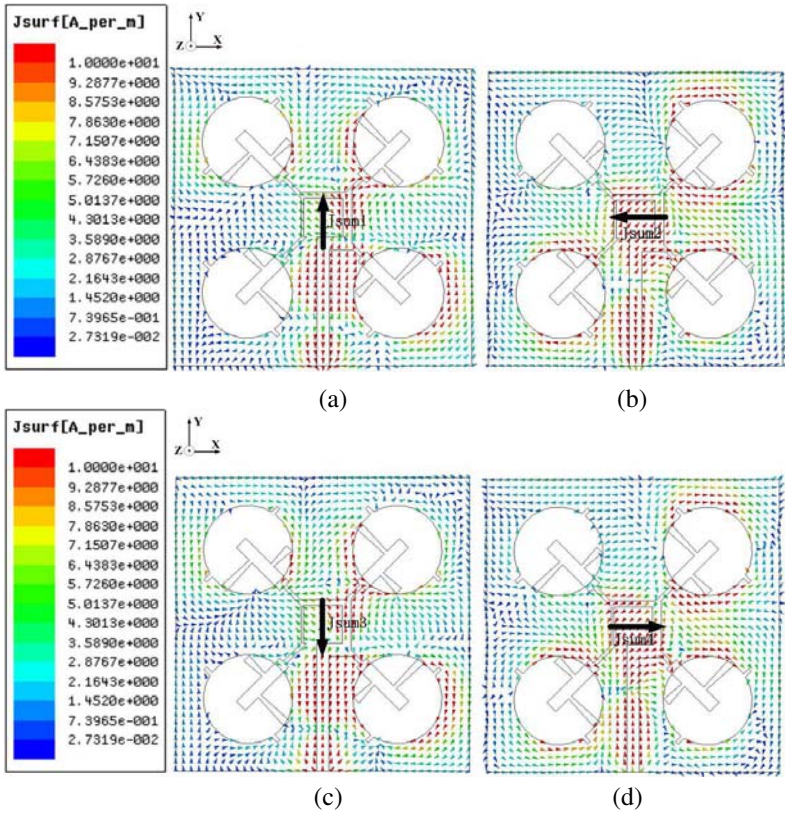

Figure 13. Current distribution at 5.8 GHz. (a) 0°, (b) 90°, (c) 180°, (d) 270°.

The proposed array has also been compared with some recently published four-element circular polarization arrays. From Table 3, we can found that the array is compact in size. Because of the one-layer structure, the array also has a low height. The array shows wide impedance bandwidth and AR bandwidth performances, which are very attractive for high speed data transmission. Considering the small size of the array, the gain is also acceptable.

Table 3. Comparison of the proposed array and other four-element arrays.

References	Total size	impedance bandwidth [GHz]	AR bandwidth [GHz]	Peak Gain [dBi]
[6]	$0.27\lambda \times 0.27\lambda \times 0.07\lambda$	0.96–1.20(22.4%)	1.062–1.137(6.8%)	5.4
[8]	$1.17\lambda \times 1.17\lambda \times 0.03\lambda$	1.76–2.64(40%)	1.83–2.65(36.6%)	8.7
[9]	$0.49\lambda \times 0.49\lambda \times 0.18\lambda$	4.85–7.2(39%)	5–6.6 (27.6%)	10
[11]	$1.45\lambda \times 1.45\lambda \times 0.03\lambda$	5.01–5.87(15.9%)	5.08–5.72(6.8%)	12.5
[12]	$1.72\lambda \times 1.72\lambda \times 0.22\lambda$	5.1–10(70%)	5.2–9.1(55%)	12.1
This Work	$0.71\lambda \times 0.71\lambda \times 0.02\lambda$	4.629.92(72.9%)	4.48–8.52(622%)	7.5

5. CONCLUSION

A sequentially fed circularly polarized antenna array with broadband performances is proposed in this paper. According to the measured results, for the four-element array the measured -10 dB impedance bandwidth is 72.9% (4.62–9.92 GHz), and 3 dB axial ratio bandwidth is 62.2% (4.48–8.52 GHz). The compact size, simple structure, wide band performances, acceptable gain, and other radiation performances show that the array is suitable for modern wireless communication systems.

REFERENCES

1. Lai, H. W., K. M. Mak, and K. F. Chan, "Novel aperture-coupled microstrip-line feed for circularly polarized patch antenna," *Progress In Electromagnetics Research*, Vol. 144, 1–9, 2014.
2. Kumar, C., M. I. Pasha, and D. Guha, "Defected ground structure integrated microstrip array antenna for improved radiation properties," *IEEE Antennas and Wireless Propagation Letters*, Vol. 16, 310–312, 2017.
3. Zhou, W., J. Liu, and Y. Long, "A broadband and high-gain planar complementary Yagi array antenna with circular polarization," *IEEE Transactions on Antennas and Propagation*, Vol. 65, No. 3, 1446–1451, March 2017.
4. Ta, S. X. and I. Park, "Compact wideband circularly polarized patch antenna array using metasurface," *IEEE Antennas and Wireless Propagation Letters*, Vol. 16, 1932–1936, 2017.
5. Rafii, V., J. Nourinia, C. Ghobadi, J. Pourahmadazar, and B. S. Virdee, "Broadband circularly polarized slot antenna array using sequentially rotated technique for C-band applications," *IEEE Antennas and Wireless Propagation Letters*, Vol. 12, 128–131, 2013.
6. Chen, X., L. Yang, J. Zhao, and G. Fu, "High-efficiency compact circularly polarized microstrip antenna with wide beamwidth for airborne communication," *IEEE Antennas and Wireless Propagation Letters*, Vol. 15, 1518–1521, 2016.
7. Fu, S., S. Fang, Z. Wang, and X. Li, "Broadband circularly polarized slot antenna array fed by asymmetric CPW for L-band applications," *IEEE Antennas and Wireless Propagation Letters*, Vol. 8, 1014–1016, 2009.
8. Feng, C. and F. Zhang, "A low-cost broadband circularly polarized antenna with integrated feeding network," *2018 IEEE MTT-S International Wireless Symposium (IWS)*, 1–4, Chengdu, 2018.

9. Nourinia, J., C. Ghobadi, and M. Majidzadeh, "Targeting wideband circular polarization: An efficient 2×2 sequentially-phase-fed rotated array antenna," *Radioengineering*, Vol. 27, 79–84, 2018.
10. Ta, S. X. and I. Park, "Metasurface-based circularly polarized patch array antenna using sequential phase feed," *2017 International Workshop on Antenna Technology: Small Antennas, Innovative Structures, and Applications (iWAT)*, 24–25, Athens, 2017.
11. Ding, K., C. Gao, T. Yu, D. Qu, and B. Zhang, "Gain-improved broadband circularly polarized antenna array with parasitic patches," *IEEE Antennas and Wireless Propagation Letters*, Vol. 16, 1468–1471, 2017
12. Bisharat, D. J., S. Liao, and Q. Xue, "Wideband unidirectional circularly polarized antenna with L-shaped radiator structure," *IEEE Antennas and Wireless Propagation Letters*, Vol. 16, 12–15, 2017.